Iranian (Iranica) Journal of Energy & Environment
Journal Homepage: wwwijeenet
IJEE an official peer review journal of Babol Noshirvani University of Technology, ISSN:2079-2115

Short Communication

Theoretical Study of Global Solar Radiation on Horizontal Area for Determination of Direct and Diffuse Solar Radiation

F. Chabane*[1,2], N. Moummi[1,2], C. Toumi[1,2], S. Boultif[1,2], A. Hecini[1,2]

[1] *Department of Mechanical Engineering, Faculty of Technology, University of Biskra 07000, Algeria*
[2] *Laboratoire de Génie Mécanique (LGM), Faculty of Technology, University of Biskra 07000, Algeria*

P A P E R I N F O

Paper history:
Received 06 May 2022
Accepted in revised form 04 July 2022

Keywords:
Chabane model
Capderou model
Diffuse
Solar energy
Solar radiation
Pollution factors

A B S T R A C T

This study aimed to compare global solar radiation on the horizontal area between two models of Chabane Foued and M.Capderou. The model of Chabane has been interested in pollution factors such as TL (turbidity), BE (Angstraon), and the chemical components of the air such as WV, O_3, CH_4, CO, CO_2, and the especial part the new pollution factor such as η_{beam}, κ_{beam}, and $\kappa_{diffuse}$, which all influenced onto solar radiation, and the model of Capderou has been used the atmospheric disturbance to calculate the direct and diffuse components of radiation received on a plane, while the constituents of the atmosphere (absorption and diffusion) can be expressed by disturbance factors, which is very necessary to determine irradiation In the clear sky. The results reveal a significant difference between the two models with approximated curves. The difference between the models probably returns to the nature of the geographic site which the authors used and injected into the models.

***doi**: 10.5829/ijee.2023.14.01.02*

NOMENCLATURE

M_{CO2}	Mole number of CO_2 (nmol)	diffuse	Diffuse of solar radiation
M_{CO}	Mole number of CO (nmol)	*I*	Direct solar radiation (W/m²)
M_{CH4}	Mole number of CH_4 (nmol)	*D*	Diffuse solar radiation (W/m²)
WV	Water vapor (cm)	Z	The altitude of the place (km)
TL	Turbidity	G	Global solar radiation (W/m²)
BE	Angstraon	**Greek Symbols**	
O_3	Ozone (Dobson)	δ	Declinaison (°)
Nj	Number of the day	κ	Constant of pollution (μmol.mol^{-1})
A_1; A_2, x_0, α	Constant of the Beam or diffuse solar radiation	η	Constant of pollution (μmol.mol^{-1})
Subscripts		φ	Latitude (°)
beam	Beam of solar radiation	ω	Hour anglar (°)

INTRODUCTION

Solar energy is the source of the most energy available on earth. It is expected to play a significant role soon, especially in developing countries. Several nations have adopted strategies and visions for the development of renewable sources to meet their energy needs and supplies. In the study of Chabane, the goal was to develop a model for predicting solar radiation that included two components: beam and diffuse solar radiation. This section of the predictive modeling looked at the relationship between the atmospheric factor and CO, CO_2, and CH_4 [1]. For the period 2015–2018, empirical estimates using sunshine duration and cloud cover as

*Corresponding Author Email: fouedmeca@hotmail.fr (F. Chabane)

Please cite this article as: F. Chabane, N. Moummi, C. Toumi, S. Boultif , A. Hecini, 2023. Theoretical Study of Global Solar Radiation on Horizontal Area for Determination of Direct and Diffuse Solar Radiation, Iranian (Iranica) Journal of Energy and Environment, 14(1), pp. 9-16. Doi: 10.5829/ijee.2023.14.01.02

input data were used to evaluate the potential of solar energy resources at 22 synoptic stations distributed across Ghana's four climatic zones (savannah, transition, forest, and coastal). The latest results revealed that the sky view factor was consistently between 0.7 and 0.8 during the dry season, with low values below 0.7 in August for all climatic zones. The savannah, coastal, and eastern transition climatic zones were observed through spatial interpolation of the sky condition parameters by Tanu et al. [2]. Yang et al. [3] chose six cities with severe pollution to examine the effect of air pollution on solar radiation (global Rs and diffuse Rd) under clear sky conditions. They discovered that Beijing had the highest levels of both global and diffuse solar radiation (Rd = 16.21 percent) and (Rs = 6.03 %) respectively [3]. Chabane et al. [4] consider a model of solar radiation which is function of latitude and longitude for each point of the Algerian map. The model provides a good estimate for the entire area of Algeria based on average solar radiation, with residual R^2= 0.981 about latitude and 0.866 longitudes. Chabane and colleagues [5] considered a model of solar radiation which is function of latitude and longitude for each point of the Algerian map. They created the correlation by analyzing sunshine and global radiation data from a meteorological station in Ghardaia for over a year. To validate and predict global solar radiation (GSR) over a horizontal surface of three Egyptian towns, Zahraa E. Mohamed used artificial neural network (ANN) models. Basic backpropagation (Bp) and Bp with momentum and learning rate coefficients are the two algorithms that are used in feedforward backpropagation ANNs [6]. P.A.Costa Rocha et al. Set out to estimate global solar radiation by presenting three ANNs that used meteorological data measured in Fortaleza as predictors [7]. Chabane et al. [8] proposed a model to predict global solar radiation contexts on a horizontal plane and other inclined areas of Biskra. The experimental results showed that the values provided a good estimate of solar radiation, which is consistent with Perrin Brichambaut's work. In the city of Biskra, Chabane et al. [9] focused on the sunlight coming to the earth and the different intensity that has a strong relationship with the number of days in the year to create a mathematical model that helps them to include all the effects of atmospheric compounds, which are CO_2 and O_3. They wanted to introduce some effects like atmospheric compounds and the angle of inclination and create another model that calculates total solar radiation as a function to direct solar radiation and diffuse solar radiation. Mihalakakou et al. [10] described a neural network approach for modeling and forecasting total solar radiation time series in the short term. In addition, an autoregressive model for analyzing and representing total solar radiation time series is developed. It was discovered while comparing predicted solar radiation values of observed data series that the neural network approach performs better than the AR model. Guermoui et al. [11] proposed a new GPR model for estimating daily global solar radiation on a horizontal surface. The Ghardadia region as a case study (Algeria). GPR - models based on sunshine duration, minimum air temperature, and relative humidity yielded the best results in terms of mean absolute bias error (MBE), root mean square error (RMSE), relative mean square error (rRMSE), and correlation coefficient (r). The goal of Chabane et al. [12] was to create a global solar radiation model based on aerosol optical depth data at two wavelengths: 550 and 1250 nm. The impact of meteorological variables like humidity, ambient temperature, and time durations was also investigated. Finally, a comparison of the theoretical and experimental results yields an excellent correlation with a low relative error that is limited to the range of 2 to 15%. This work allowed for a comparison study of Chabane's model and Capderou's model for calculating solar radiation.

In this numerical and experimental work in the city of Biskra at a mean constant solar radiation I= 869 W/m², Z. Aouissi et al. [13] created a dynamics model (CFD) that matches the experimental model at the same experimental conditions. Utilizing a solar heat collector by improving the heat transfer inside it by incorporating rectangular flaps in the middle Passage of distributed air at different angles of inclination[13]. Mahmoudi et al. [14] conducted an experimental study of using aluminum sawdust as an asphalt coating material to improve its thermal performance and built a crooked (SAH) prototype with the use of many sensors to monitor its thermodynamic response. Thus, they found that the coating strategy improved the thermal efficiency by 22.74% and 44% in 2 air mass flow rates. Ameri et al. [15] were also interested in a current experimental study of different coverage strategies to construct two models of solar air heaters (SAHs), with one acrylic cover, one glass cover, and a double glass cover. Therefore, they concluded during the experimental operation that the double-covered SAH is higher and improves the resistance to solar radiation, in contrast to the acrylic panel, which is resistant to harsh ambient conditions only. In this study, Bagheri Sabzevar and Erfan [16] carried out a year in three rooms, on three floors of the office building of Hakim Sabzivari University with window openings of different depths and angles that allow solar radiation to pass through while reducing the amount of energy consumed to find the optimum shading features. Fixed louvers for the eastern and western facades and South simulate distances using software for optimization. A Gunn-Bellani radiometer was used to collect data on global solar radiation for Ikeja [17]. A linear regression, correlation model was developed for Ikeja and other nearby areas in Nigeria's southwest with similar meteorological conditions. The global solar radiation estimates were then based on test results, and statistical test results [MBE, RMSE, MPE] and confirmed to be precise. The clearness index value was also estimated at approximately 0.31 to 0.59,

suggesting that Lagos has a partly clear sky. In the constructed double slope [18], the solar distillery was used to obtain brackish water from a local dirty stream that experiences throughout the year. The sun's incoming solar radiation is concentrated and confined to the solar water distillation unit. The pH value of the brackish feed water was 9.2, while that of the distillate was 8.1 both of which fall within who limits of 6.5-8.5 for drinkable water. Bensahal and Yousfi [19], are working on an hourly air temperature estimation model (MAT) based on available meteorological measured data from Laghouat (Algeria) Predicated on atmospheric pressure, global solar radiation, and relative humidity data, the current model can calculate the hourly air temperature at any time of day or night. This work was compared to three published models in the literature, namely the Wave, Idliman, and Double cosine. The estimated and measured results were compared using statistical parameter tests such as the mean bias error (MBE), mean percentage error (MPE), mean absolute error (MAE), RMSE, and coefficient of determination (R^2). In some work the researchers [20] used ARIMA models to simulate solar irradiance in nine Nigerian locations. Findings revealed that in Kebbi, Iwo, and Maiduguri, the best forecasting ARIMA was (3,0,3), in Calabar as well as Sokoto, it was ARIMA (2,0,2), and in other study areas like Enugu, Ikeja, Ilorin, and Port Harcourt, ARIMA (2,0,3) was the better model for forecasting irradiance. However, it is concluded that the predicted irradiance values between January 2020 and December 2020, along with their respective 95% confidence level, indicate a great estimate of solar irradiance for future occurrences.

In this research, Gandjalikhan and Addini [21] proposed employing radiating gas instead of air inside the cavity of compound parabolic collectors (CPSs), and demonstrate this numerical analysis using the finite element method (FEM) using the COMSOL multi-physics. It was found that the gas radiation raises the temperature inside the collector's cavity with a more even distribution. Additionally, numerical findings show a greater than 3% increase in the rate of heat transfer from the absorber surface into the working fluid.

In this study, Aweda et al. [22] calculated the net radiation using a straightforward expression that is based on the Fourier Series Technique's basic tenets. It demonstrates the major impact of temperature and solar radiation on net radiation.

Chabane et al., [12]were developed a mathematical model of global solar radiation that depends on the aerosol optical depth data between two wavelengths, Chabane et al. [12] measured and modeled solar radiation on the horizontal area. Samson et al. [23] used daily data from numerous locations to examine the extraterrestrial radiation on the earth's surface during the year 2018. Sokoto and Maiduguri had the highest solar radiation, according to the results, which were then drawn from.

MATERIAL AND METHODS

In this comparative study, Chabane Foued's method developed a model to predict solar radiation on a horizontal area, taking into consideration the different contexts and added air pollutants such as CO, CO_2, and CH_4 linked to factors such as η_{beam}, k_{beam}, $k_{diffuse}$ β, T_L, and Capderou's method is based on the use of atmospheric disturbance to calculate the direct and diffuse components of radiation received in a plane, using an atmospheric model. The model expresses direct and diffuse clear sky irradiations as a function of disturbance factors.

Geographical location

Biskra, the desert gate, is located at the foot of the Aurès massif's southern slope. It is the first stage and the doorway to the Saharan area, located in eastern Algeria at the junction of two valleys that cross the massif. Biskra's strategic location has made it a natural relay for north-south trade, in addition to the water and soil resources that have supported agriculture.

The Wilaya of Biskra is 21,671.2 km^2 Long, with the Wilaya of Batna to the north, the Wilaya of M'sila to the north-west, the Wilaya of Khenchela to the north-east, the Wilaya of El Oued to the south, and the Wilaya of Djelfa to the south-west. Biskra is located at 34°48' north latitude and 05°44' east longitude.

Theoretical studies

Astronomic parameter

- *The direction of solar radiation*

To locate the position of the sun in the sky, it is useful to use a system of local coordinates (azimuthal coordinates) defined as a point on the Earth's surface (located in the northern hemisphere). Its axes are defined as follows:

OX towards the south, OY towards the west, and OZ vertical of the place, upwards. the direction (OS) of the sun is marked by two angles:

height sun h: Angle between the astronomical horizon and the axis from the point considered to the sun. It is counted from 0° to 90° if the sun is in the southern hemisphere (Nadir).

azimuth a: Angle between the projection of the direction of the sun (OS) on the horizontal plane and the south, it is counted positively towards the west and negatively towards the east.

declination (δ): Angle between the direction of the sun and the equatorial plane of the earth or the latitude of the place where the sun is vertical at solar noon.

$$\sin \delta = 0.398 \sin [0.986 (Nj-82)]$$
$$\text{either } \delta = 23.45 \sin [0.986 (284 + Nj)] \quad (1)$$

The hour angle (ω): between the planes (OZ', OS) and (OZ', OX'): The hour angle is formed by the meridian plane passing through the center of the sun and the vertical plane of the place. At solar noon the hour angle

(ω) is equal to 0°, then each hour corresponds to 15° because the earth makes a full turn (360°) on itself in 24 hours. The angle (ω) is counted negatively in the morning when the sun is towards the East and positively after the solar midday.

In practice, we express the angles (h) and (a) according to the latitude of the place, the declination, and the hour angle of the sun: sinh = cos ϕ cos δ cos ω + sin ϕ sin δ and:

$$\sin(a) = \frac{\cos(\delta).\sin(\omega)}{\cos(h)} \quad (2)$$

Duration of the day: The value ω_l of the time angle at sunrise is obtained by considering sinh null because the height of the sun is equal to 0 at sunrise and sunset, which leads to writing:

$$\cos(\omega_l) = -\tan(L)\tan(\delta) \quad (3)$$

The solar time at sunrise is, therefore:

$$(TS)_l = 12 - {}^{\omega_l}\!/_{15} \quad (4)$$

The hour angle ωc at sunset is the opposite of the hour angle at sunrise, so:

ωc = -ωl and the duration of the day is: $d = 2\frac{\omega_l}{15}$

Different models of the solar radiation

- *Model Chabane (horizontal area)*

The pollution factor it's an important parameter to be determined by the turbidity factor, CO_2, CO, and CH_4 were all crucial characteristics that were incorporated into his model. He has compiled a list of studies related to this form of research, which is linked to contaminated components and sunshine prediction equations.

The real results are taken from the Assekrem area in Algeria. He has chosen the nonlinear equation in the form of an exponential function for the investigation of the diffuse and direct solar radiation yields the shape of the exponential function with a change in the angle of the solar elevation.

Chabane decided to find and define a mathematical model to determine the global solar radiation on the horizontal area as a function of h, CO_2, CO, and CH_4 using the obtained experimental data. Pollution terms can be written as a function of the number of days:

$$M_{CO2} = 404.264 + 3.561 \times \sin\left(\pi \times \left(\frac{Nj - 36.307}{146.31}\right)\right) \quad (5)$$

$$M_{CH4} = \exp\left(\begin{matrix} 7.5413 - 1.1963 \times 10^{-4} \times Nj + \\ 3.7968 \times 10^{-7} \times Nj^2 \end{matrix}\right) \quad (6)$$

$$M_{CO} = 101.43 + 16.06 \times \sin\left(\pi \times \left(\frac{Nj + 20.3}{180.52}\right)\right) \quad (7)$$

Table 1 shows different constants of the prediction model of the beam solar radiation, according to the pollution elements of CO_2 CO and CH_4.

$$Beam = A_2 + \frac{(A_1 - A_2)}{1 + \exp\left(\frac{h - \left(\frac{T_L}{10} + \eta_{beam}\right)}{\beta - \kappa_{beam}}\right)} \quad (8)$$

The values of β and T_L estimate the new pollution parameters and Linke turbidity factor, respectively, which is scripted by the relationship as follows:

$$T_L = 8.055 \times O_3^{0.0104} \times WV^{0.128} \times BE^{0.295} \quad R^2 = 0.986 \quad (9)$$

The turbidity factor as a function of ozone, water vapor, and Angstrom coefficient, can be determined and is presented in Table 2.

Table 1. The constant of the Beam solar radiation

Month	A_1	A_2	x_0	α
January	-5.837	878.4105	0.44582	0.16727
February	-7.608	980.5861	0.49865	0.18991
March	-11.71	1098.745	0.54277	0.21467
April	-15.77	1121.657	0.58337	0.23133
May	-16.29	1009.154	0.61971	0.23545
June	-18.38	1019.735	0.61365	0.23587
July	-18.22	1043.801	0.60945	0.23664
August	-14.17	991.0254	062201	0.23246
September	-11.58	999.3427	0.58321	0.21799
October	-8.214	933.4700	0.53671	0.19544
November	-6.306	886.2020	0.47012	0.17189
December	-5.276	828.0225	0.43172	0.15609

Table 2. The atmospheric element of the pollution

Month	TL	O_3	WV	BE
1	2.7	263	0.64	0.02
2	2.5	270	0.64	0.02
3	3.1	255	0.71	0.04
4	3.2	272	0.81	0.04
5	3.1	272	1.05	0.03
6	3.8	278	1.31	0.06
7	3.8	274	1.23	0.06
8	4.2	273	1.24	0.08
9	4.3	262	1.21	0.09
10	4.4	257	0.97	0.1
11	3.3	254	0.77	0.05
12	3.7	253	0.67	0.07

Table 2 shows the different atmospheric elements of pollution, which were determined by turbidity factor, ozone, water vapor, Angstrom coefficient, and the new atmospheric element of the pollution according to the new mathematical model of the beam and diffuse solar radiation.

$$\beta = 0.1 \times \frac{M_{co} + M_{CO_2} + M_{CH_4}}{10^3} - \beta_0 \quad R^2 = 0.9996 \tag{10}$$

η_{beam} and κ_{beam} represent the new coefficients of the pollution corresponding to beam solar radiation, according to β and T_L, respectively, written according to the relationship as follows:

$$\eta_{beam} = \eta_0 \times T_L^{5.25} \times \beta^{-0.1388} \quad R^2 = 0.9222 \tag{11}$$

η_0 constant of the coefficient of η_{beam} depending on the beam solar radiation, and equal to 0.0000429 $(\mu mol.mol^{-1})^{1.4}$.

$$\kappa_{beam} = \kappa_0 \times T_L^{-0.702} \times \beta^{1.678} \quad R^2 = 0.984 \tag{12}$$

κ_0 constant of the coefficient of κ_{beam} related with the beam solar radiation equal to 2.396 $(\mu mol.mol^{-1})^{0.8}$.

The global solar radiation writes by beam and diffuse solar radiation and the diffuse solar radiation is estimated as follows:

$$Diffuse = A_2 + \frac{\left(\left(\frac{T_L}{10} + \kappa_{diffuse}\right) - A_2\right)}{1 + \exp\left(\frac{h - x_0}{\alpha}\right)} \tag{13}$$

$$\kappa_{diffuse} = \kappa_1 \times T_L^{6.868} \times \beta^{-0.184} \quad R^2 = 0.893 \tag{14}$$

k_1 the constant of the coefficient of κ_{diffuse} relates to diffuse solar radiation equal to −0.0000545 $(\mu mol.mol^{-1})^{1.2}$.

Table 3. The constants of the diffuse solar radiation

Month	A_1	A_2	x_0	α	R^2
1	-0.509	57.944	0.1674	0.1210	0.98
2	-0.589	77.5126	0.1717	0.1254	0.96
3	-0.636	66.8094	0.1837	0.1324	0.97
4	-0.789	69.5116	0.1864	0.1308	0.98
5	-2.328	120.335	0.2558	0.1617	0.99
6	-2.368	110.672	0.245	0.1586	0.98
7	-1.678	92.1492	0.2222	0.1480	0.98
8	-1.909	120.309	0.2603	0.1598	0.98
9	-1.177	93.7809	0.2398	0.1496	0.99
10	-1.186	93.5517	0.2294	0.1460	0.98
11	-0.727	69.8516	0.1916	0.128	0.99
12	-0.507	62.8979	0.1715	0.1152	0.99

- *Model Capderou (horizontal and incline area)*

The Capderou model uses the coefficient of atmospheric disturbance to calculate the direct and diffuse components of the radiation received in a plane.

In this model, the light sky Linke atmospheric disturbance factor is given by:

$$T_L^* = T_0 + T_1 + T_2 \tag{15}$$

T_0 is the disturbance factor due to the gaseous absorption by both the fixed constituents of the atmosphere and by ozone and especially by water vapor. Modeling of this factor, according to Geo-astronomical parameters alone allowed Capderou to propose the following expression:

$$T_0 = 2.4 - 0.9\sin(\varphi) + 0.1(2 + \sin(\varphi))A_{he} - 0.2Z - (1.22 + 0.14A_{he})(1 - \sin(h)) \tag{16}$$

$$A_{he} = \sin\left(\left(\frac{360}{365}\right)(j - 121)\right) \tag{17}$$

where Z is the altitude of the place.

T_1 is the coefficient of disorder corresponding to the absorption by gases in the atmosphere (O_2, CO_2, and O_3) and the molecular diffusion Rayleigh given by:
For a day one can simulate its variation from sunrise to sunset.

T_2 is the disturbance factor related to diffusion by aerosols coupled with slight absorption (it depends on both the nature and quantity of aerosols). T_2 is given by:

$$T_2 = (0.9 + 0.4A_{he})(0.63)^Z \tag{18}$$

The direct illuminance in a clear sky, on a horizontal plane, is given by:

$$I = I_0 \sin(h) C_{ts} \exp\left[-T_L^*\left(0.9 + \frac{9.4}{0.89^Z}\sin(h)\right)^{-1}\right] \tag{19}$$

Incident diffuses illuminance on a horizontal plane:

$$D = I_0 C_{ts} \exp(-1 + 1.06\log(\sin(h))) + a - \sqrt{a^2 + b^2} \tag{20}$$

$$a = 1.1 \quad b = \log(T_L^* - T_0) - 2.8 + 1.02(1 - \sin(h))^2 \tag{21}$$

For a day one can simulate its variation from sunrise to sunset. The global illuminance received on a horizontal plane is given by: G =I +D

RESULTS AND DISCUSSION

Figure 4 shows the variation of components of solar radiation of model Chabane as a function of time of the day according to horizontal area. The solar radiation of direct, diffuse, and global began with low radiation, which approximates the sunrise, and then increased to a maximum elevation, which is estimated to be midday at

12h00, and then decreased to low graduate values to minimum radiation, which approximates the radiation of the sunset. The diffuse solar radiation does not exceed 100 W.m^{-2} while the direct solar radiation follows a similar curve to the global solar radiation but has lower values.

Figure 5 shows the variation of components of solar radiation of model Capderou as a function of time of the day according to horizontal area. The solar radiation of direct, diffuse, and global started with low radiation, which means that approximates the sunrise and takes a maximum elevation which is estimated to midday at 12h00, and then the curves of solar radiation decrease with low graduate values to minimum radiation, which means the variation, approximate the radiation of the sunset.

The diffuse solar radiation takes values does not exceed 100 W.m^{-2}, and the direct solar radiation varies with a similar evolution of the global solar radiation but with higher values.

Figure 6 shows the global solar radiation with model Foued Chabane and model M.Capderou, as a function of the time of the day according to horizontal area. The global solar radiation takes values do not exceed the 1000 W.m^{-2}, and the global solar radiation of model Foued Chabane varies with a similar evolution to the global solar radiation of model M.Capderou but with lower values. The curves intersect at a point that does not exceed 350 W.m^{-2}.

Figure 7 represents the scatter chart between the global solar radiation model Capderou and the global solar radiation model Foued Chabane according to the horizontal area, and we can see that The goal of this section of the curve is to show how to approximate the data calculation of both models of near and far linear lines with perfect tilt angles, which approach 1 and the linear line's evolution began with 0.

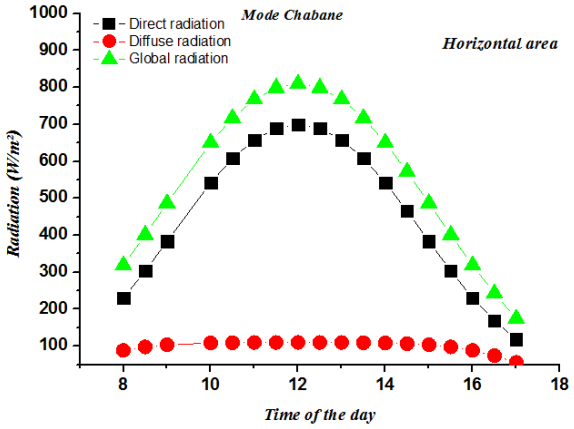

Figure 4. Solar radiations with components direct, diffuse, and global, corresponding to model Chabane (16.06.2022)

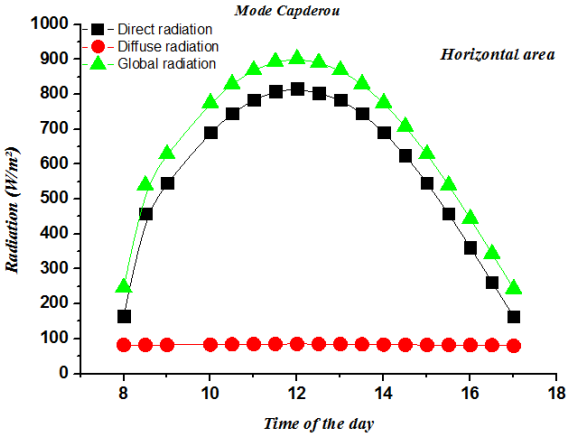

Figure 5. Solar radiation with components direct, diffuse, and global, corresponding to model Capderou

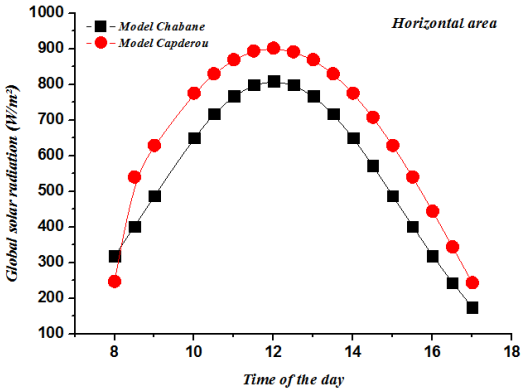

Figure 6. Global solar radiation with model Chabane and model Capderou, on a horizontal area

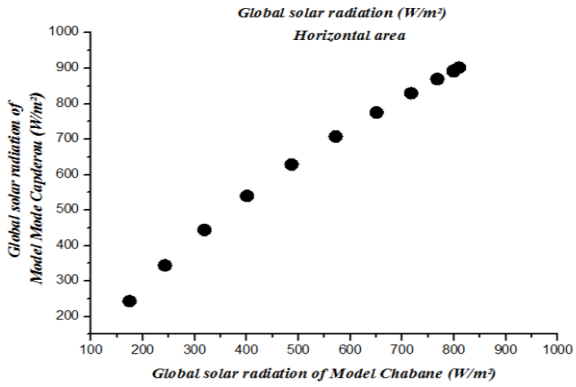

Figure 7. Global solar radiation model Capderou

CONCLUSION

Through the calculation of the solar radiation, we conclude that the Chabane model is based on the pollution

parameters (CO, CO_2, CH_4, O_3, and the water vapor) while the Capderou model uses the disturbance factor TL, and both models in the condition with clear sky. Both models depend on climate conditions, which is considered an important factor in influencing global solar radiation.

According to the results of the global solar radiation, we observed that the evolution of the curves is approximate with acceptable values. Finally, we conclude that the difference between the models probably returns to the nature of the geographic site which the authors used and injected into the models.

REFERENCES

1. Chabane, F., 2020. Estimation of direct and diffuse solar radiation on the horizontal plane considering air quality index and turbidity factor in Assekrem, Tamanrasset, Algeria, *Air Quality, Atmosphere & Health*, 13(12), pp. 1505-1516. Doi:10.1007/s11869-020-00904-9
2. Tanu, M., Amponsah, W., Yahaya, B., Bessah, E., Ansah, S. O., Wemegah, C. S. and Agyare, W. A., 2021. Evaluation of global solar radiation, cloudiness index and sky view factor as potential indicators of Ghana's solar energy resource, *Scientific African*, 14, pp. e01061. Doi:10.1016/j.sciaf.2021.e01061
3. Yang, L., Gao, X., Li, Z. and Jia, D., 2022. Quantitative effects of air pollution on regional daily global and diffuse solar radiation under clear sky conditions, *Energy Reports*, 8, pp. 1935-1948. Doi:10.1016/j.egyr.2021.12.081
4. Chabane, F., Arif, A. and Benramache, S., 2020. Prediction of the solar radiation map on Algeria by latitude and longitude coordinates, *TECNICA ITALIANA-Italian Journal of Engineering Science*, 64(2-4), pp. 213-215. Doi:10.18280/ti-ijes.642-413
5. Chabane, F., Moummi, N. and Brima, A., 2016. Predictions of solar radiation distribution: Global, direct and diffuse light on horizontal surface, *The European Physical Journal Plus*, 131(4), pp. 1-8. Doi:10.1140/epjp/i2016-16106-7
6. Mohamed, Z. E., 2019. Using the artificial neural networks for prediction and validating solar radiation, *Journal of the Egyptian Mathematical Society*, 27(1), pp. 1-13. Doi:10.1186/s42787-019-0043-8
7. Rocha, P., Fernandes, J., Modolo, A., Lima, R., da Silva, M. and Bezerra, C., 2019. Estimation of daily, weekly and monthly global solar radiation using ANNs and a long data set: a case study of Fortaleza, in Brazilian Northeast region, *International Journal of Energy and Environmental Engineering*, 10(3), pp. 319-334. Doi:10.1007/s40095-019-0313-0
8. Chabane, F., Guellai, F., Michraoui, M.-Y., Bensahal, D., Bima, A. and Moummi, N., 2019. Prediction of the global solar radiation on inclined area, *Applied Solar Energy*, 55(1), pp. 41-47. Doi:10.3103/S0003701X19010055
9. Chabane, F., Moummi, N. and Brima, A., 2021. A New Approach to Estimate the Distribution of Solar Radiation Using Linke Turbidity Factor and Tilt Angle, *Iranian Journal of Science and Technology, Transactions of Mechanical Engineering*, 45(2), pp. 523-534. Doi:10.1007/s40997-020-00382-5
10. Mihalakakou, G., Santamouris, M. and Asimakopoulos, D., 2000. The total solar radiation time series simulation in Athens, using neural networks, *Theoretical and Applied Climatology*, 66(3), pp. 185-197. Doi:10.1007/s007040070024
11. Guermoui, M., Gairaa, K., Rabehi, A., Djafer, D. and Benkaciali, S., 2018. Estimation of the daily global solar radiation based on the Gaussian process regression methodology in the Saharan climate, *The European Physical Journal Plus*, 133(6), pp. 1-17. Doi:10.1140/epjp/i2018-12029-7
12. Chabane, F., Arif, A., Moummi, N. and Brima, A., 2020. Prediction of Solar Radiation According to Aerosol Optical Depth, *Iranian (Iranica) Journal of Energy & Environment*, 11(4), pp. 271-276. Doi:10.5829/ijee.2020.11.04.04
13. Aouissi, Z., Chabane, F., Teguia, M.-S., Belghar, N., Moummi, N. and Brima, A., 2022. Optimization of the heat exchange by adding the baffles to the streaming duct of the solar air collector, *Iranian (Iranica) Journal of Energy & Environment*. Doi:10.5829/ijee.2022.13.04.04
14. Mahmoudi, M., Farzan, H. and Hasan Zaim, E., 2022. Performance of New Absorber Coating Strategy in Solar Air Heaters: An Experimental Case Study, *Iranian (Iranica) Journal of Energy & Environment*, 13(2), pp. 124-133. Doi:10.5829/ijee.2022.13.02.03
15. Ameri, M., Farzan, H. and Nobari, M., 2021. Evaluation of different glazing materials, strategies, and configurations in flat plate collectors using glass and acrylic covers: An experimental assessment, *Iranian (Iranica) Journal of Energy & Environment*, 12(4), pp. 297-306. Doi:10.5829/ijee.2021.12.04.03
16. Bagheri Sabzevar, H. and Erfan, Z., 2021. Effect of Fixed Louver Shading Devices on Thermal Efficiency, *Iranian (Iranica) Journal of Energy & Environment*, 12(4), pp. 349-357. Doi:10.5829/ijee.2021.12.04.08
17. Nathaniel, O. A., Oluwadara, A. S., Joshua, O. A. and Jacob, A. A., 2019. Estimation of global solar radiation and clearness index in coast of Gulf of Guinea, Nigeria, *Iranian (Iranica) Journal of Energy & Environment*, 10(3), pp. 211-215. Doi:10.5829/ijee.2019.10.03.08
18. Oyewole, J. and Olanrewaju, A., 2019. Performance of a Double Slope Solar Water Distillation: A Case Study of Aiba Stream in Iwo, *Iranian (Iranica) Journal of Energy & Environment*, 10(2), pp. 111-114. Doi:10.5829/ijee.2019.10.02.07
19. Bensahal, D. and Yousfi, A., 2018. Hourly air temperature modeling based on atmospheric pressure, global solar radiation and relative humidity data, *Iranian (Iranica) Journal of Energy & Environment*, 9(2), pp. 78-85. Doi:10.5829/ijee.2018.09.02.01
20. Aweda, F. and Samson, T., 2020. Modelling the Earth's Solar Irradiance Across Some Selected Stations in Sub-Sahara Region of Africa, *Iranian (Iranica) Journal of Energy & Environment*, 11(3), pp. 204-211. Doi:10.5829/ijee.2020.11.03.05
21. Gandjalikhan Nassab, S. and Moein Addini, M., 2021. Effect of Radiative Filling Gas in Compound Parabolic Solar Energy Collectors, *Iranian (Iranica) Journal of Energy & Environment*, 12(3), pp. 181-191. Doi:10.5829/IJEE.2021.12.03.01
22. Aweda, F., Adebayo, S., Samson, T. and Ojedokun, I., 2021. Modelling net radiative measurement of meteorological parameters using merra-2 data in sub-sahara african town, *Iranian (Iranica) Journal of Energy & Environment*, 12(2), pp. 173-180. Doi:10.5829/IJEE.2021.12.02.10
23. Aweda, F., Oyewole, J., Fashae, J. and Samson, T., 2020. Variation of the Earth's Irradiance over Some Selected Towns in Nigeria, *Iranian (Iranica) Journal of Energy & Environment*, 11(4), pp. 301-307. Doi:10.5829/ijee.2020.11.04.08

Persian Abstract

چکیده

این مطالعه با هدف مقایسه تابش جهانی خورشید در سطح افقی بین دو مدل Chabane Foued و M.Capderou انجام شد. هوا مانند WV، O_3، CH_4، CO، CO_2 و بخش ویژه عامل آلودگی جدید مانند پرتو، پرتو و انتشار که همگی بر تابش خورشید تأثیر می‌گذارند و در این پژوهش از مدل کاپدرو استفاده شده است. اغتشاش اتمسفر برای محاسبه مولفه‌های مستقیم و پراکنده تابش دریافتی در یک هواپیما، در حالی که اجزای تشکیل‌دهنده جو (جذب و انتشار) را می‌توان با عوامل اغتشاش بیان کرد که برای تعیین تابش در آسمان صاف بسیار ضروری است. نتایج نشان می‌دهد که تفاوت معناداری بین دو مدل با منحنی‌های تقریبی وجود دارد.